2. Reduced-gravity models of the tropical ocean. The long-wave approximation.

One of the main theoretical tools for understanding the ocean dynamics in the tropics is the shallow-water models of the ocean. These models employ the fact that the thermocline can be considered a boundary separating two fluids with different densities (Figure 11). Here I give a description of a simple ($1\frac{1}{2}$-layer) version of such models.

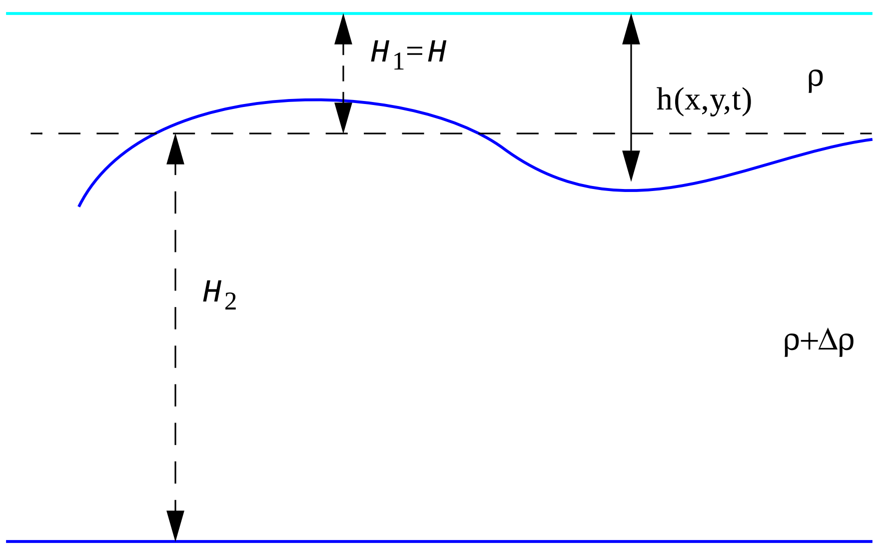

Figure 11. A schematic sketch of a two-layer fluid

For simplicity, symmetry with respect to the equator, no meridional winds, and no annual forcing are assumed. We also require that $H_1 \ll H_2$. This allows us to disregard the motion in the lower layer (perhaps, that is why the approximation is called $1\frac{1}{2}$-layer).

The momentum and mass conservation equations in this approximation are

$$u_t + g'h_x - \beta y v = -ru + \frac{\tau}{\rho H}, \tag{2.1}$$

$$g'h_y + \beta y u = 0. \tag{2.2}$$

$$h_t + H(u_x + v_y) = -rh, \tag{2.3}$$

The notation is conventional with positive $h(x, y, t)$ denoting the total local depth of the thermocline, $u(x, y, t)$ the zonal velocity, $v(x, y, t)$ the meridional velocity, $\tau(x, y, t)$ the zonal wind stress, d the depth characterizing the effect of wind on the thermocline, ρ the mean water density, H the mean depth of the thermocline, r the linear Raleigh damping, and g' the reduced gravity

$$g' = \frac{\Delta\rho}{\rho} g. \tag{2.4}$$

The standard no-flow boundary condition is usually applied at the eastern ocean boundary

$$u = 0 \qquad \text{at} \qquad x = x_E$$

and the zero-net-flow condition at the western boundary

$$\int u\,dy = 0 \qquad \text{at} \qquad x = x_W$$

Some of the assumptions used in the derivations are:

1) Long waves approximation. The scales of motion are comparable with the size of the basin.
2) The "rigid-lid" approximation. The changes in the see level are small.
3) Nonlinearities are unimportant.
4) The equatorial β-plane approximation.

With a proper choice of the zonal wind stress these equations can describe relatively well both the mean state of the ocean (Figure 12) and its variations. Yet, there are certain deficiencies in the model. For instance, the system (2.1)-(2.5) can not describe the Equatorial undercurrent. Using the $2\frac{1}{2}$-layer models improves the situation, but usually the original $1\frac{1}{2}$-layer approximation is usually sufficient for many applications.

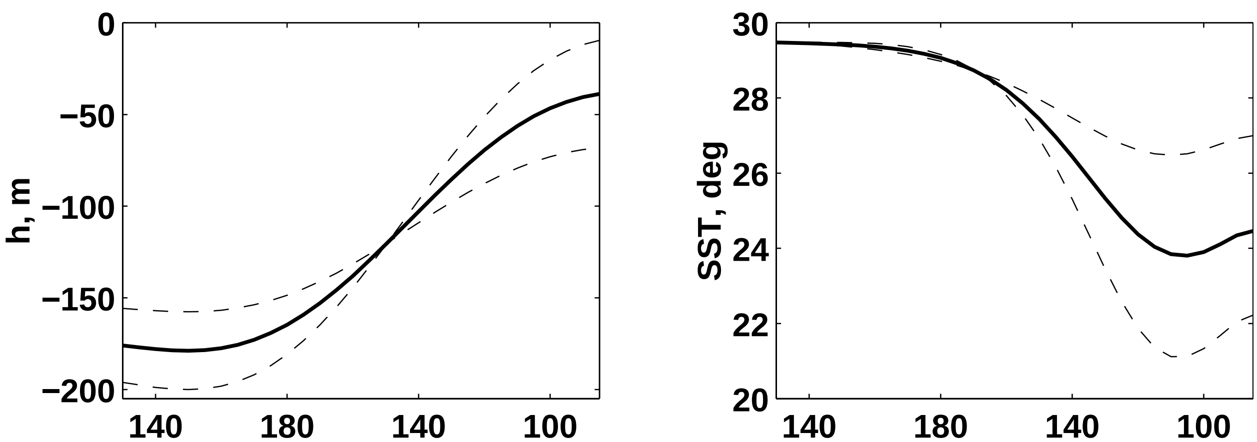

Figure 12. A typical mean state calculated by a shallow water model (solid lines) with an added SST equation, and examples for slightly different winds (dashed lines).

Equations (2.1) - (2.3) can be nondimensionalized if one introduces an important parameter - the Rossby radius of deformation

$Ro = \sqrt{c/\beta}$

where

$c = \sqrt{g'H}$.

It turns out that c is the fastest speed with which waves can propagate along the thermocline (eastward), while the Rossby radius Ro determines the characteristic scale of disturbances trapped on the equatorial thermocline (see the Appendix). In the equatorial ocean $Ro \approx 300km$.

3. Ocean Adjustment

3.1. Free equatorial waves. Kelvin and Rossby waves. Ocean response to wind bursts.

In this section I wanted to come up with something new, but unfortunately, the theory is rather complete and it is difficult to invent something new. So I have confined myself to a brief introduction, but for completeness, I add an Appendix with detailed derivations from Eli Tziperman lectures for Woods Hole GFD 2001 (these derivations closely follow Gills (1982) approach).

To describe the ocean adjustment under varying wind forcing we must solve Eq. (2.1)-(2.5). A solution of these equations can be presented as a sum of Kelvin and Rossby waves.

A Kelvin wave propagates eastward with the phase speed c (~2.6 m/s). It takes about 2 months for a Kelvin wave to cross the Pacific ocean. A Kelvin wave induces a large displacement of the thermocline at the equator, and decay off-the equator with the exponential decay scale proportional to the Rossby radius. Kelvin waves produce no meridional flow, i.e. $v=0$;

There are infinite number of Rossby waves. They propagate westward with the phase speeds $c/3, c/5, c/7, c/9, \ldots$ It takes about 6 months for the fastest Rossby wave to cross the Pacific ocean. The largest signature of Rossby waves is off the equator. The spacial structure of the Kelvin and the first Rossby wave is shown in Figure 13.

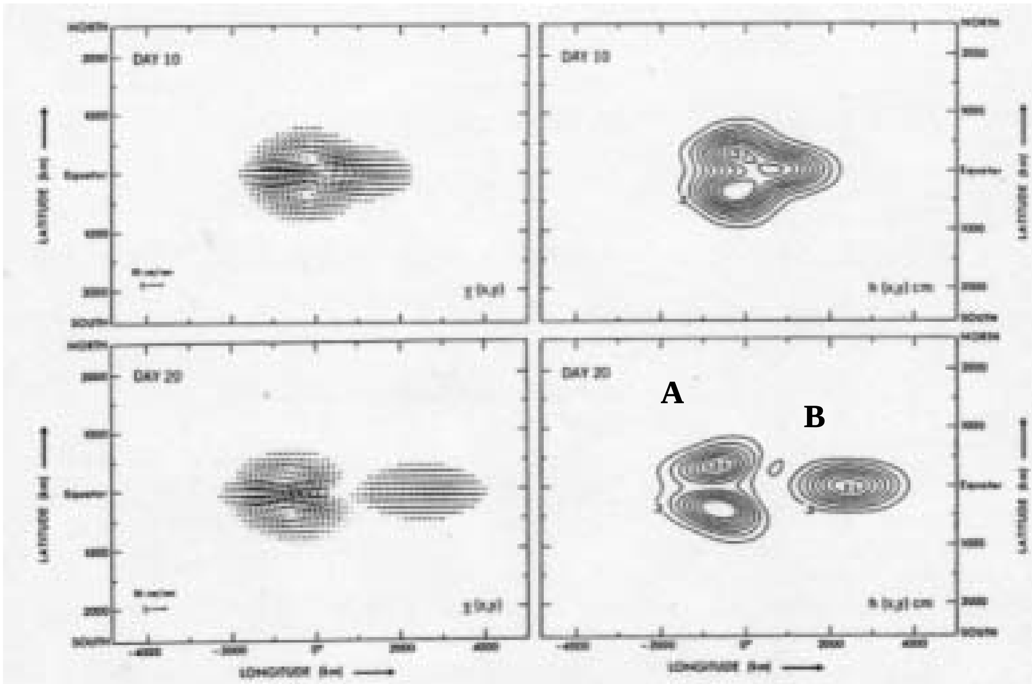

Figure 13. The generation of a Kelvin waves (B) and a Rossby wave (A) on the thermocline from an initial disturbance (or after a sudden wind burst). Both velocity and thermocline anomalies are shown

3.2. Ocean response to slowly-varying periodic winds. The ocean “memory”

When the wind stress is varying interannual the response of the ocean still resembles the Kelvin-Rossby wave response (Figure 14), but now it is a superposition of infinite number of Kelvin and the first and higher-order Rossby waves.

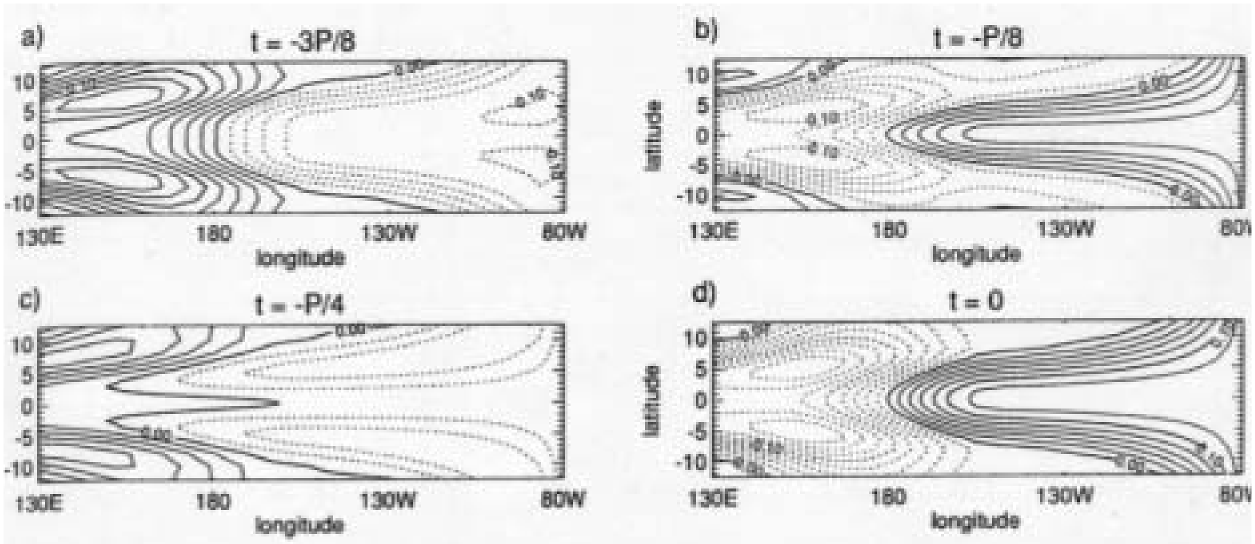

Figure 14. Typical changes in the thermocline depth associated with slow changes in the winds. The wind variations are sine-like and have the period P=3years. The structure of the thermocline anomalies at four different times is shown.

Importantly, the balance between the wind and the thermocline slope establishes very fast along the equator, so that the x-momentum equation at the equator becomes

$$g'h_x \approx \frac{\tau}{\rho H}.$$

Off the equator, where the slower Rossby waves do all the job, the adjustment is much slower, so that the ocean “remembers” changes in the zonal wind stress for some time. It is this ocean memory that allows for continuous oscillations in the coupled system - an unbalanced perturbation off the equator may induce a perturbation along the equator changing conditions in the eastern Pacific and initiating ocean-atmosphere interactions (amounting to strong positive feedbacks).

One can combine the results of calculations shown in Figure 14 to produce a time-longitude diagram (a Hovemoller diagram) of the thermocline changes along the equator.

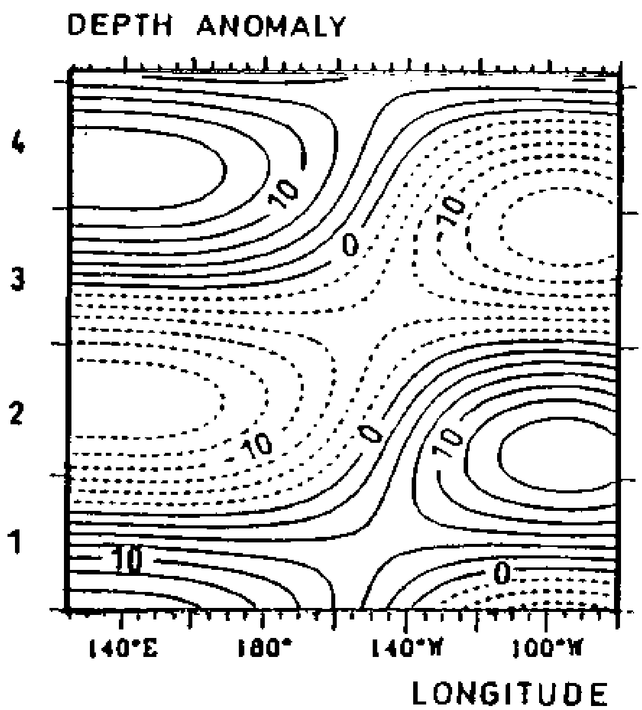

Figure 15. A Hovemoller diagram of thermocline changes along the equator that correspond to spacial variation depicted in Figure 14. The time (i.e. the vertical axes) is in years. Further, please compare Figures 14 and 15 with Figures 18 and 19.

3.3. Ocean response to cross-equatorial winds.

So far I have been neglecting the fact that the background state of the tropical ocean is actually asymmetric with respect with the equator. To take the asymmetry into account an extra term should be added in the shallow-water equations

$$g'h_y + \beta y u = \tau^y / \rho H,$$

where τ^y is the meridional wind stress.

Surprisingly, if one applies such meridional stress to the ocean, the SST pattern in the eastern Pacific will look similar to the observations (Figure 16). The reason for this is that the northward wind stress along the coast creates upwelling in the Southern hemisphere and also creates the south-north thermocline slope. Together these two effects contribute to the strength of the cold tongue in the eastern Pacific.

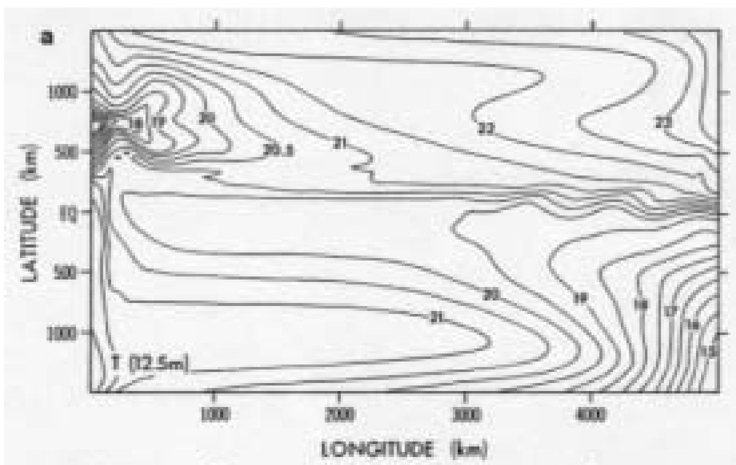

Figure 16. An SST pattern produced by southerly wind stress (uniform and constant in space).

When the zonal winds relax, so do the meridional winds, so that during El Niño the asymmetry all but disappears. This effect strengthens El Niño and also result in several important atmospheric phenomena, including the southward migration of ITCZ.